J. Gen. Appl. Microbiol., **63**, 305–309 (2017)
doi 10.2323/jgam.2017.02.002

jGAM

Short Communication

Construction of a rapamycin-susceptible strain of the unicellular red alga *Cyanidioschyzon merolae* for analysis of the target of rapamycin (TOR) function

(Received December 3, 2016; Accepted February 2, 2017; J-STAGE Advance publication date: September 26, 2017)

Sousuke Imamura,[1,2,*] Keiko Taki,[1,2] and Kan Tanaka[1,2,*]

[1] *Laboratory for Chemistry and Life Science, Institute of Innovative Research, Tokyo Institute of Technology, Yokohama, Japan*
[2] *Core Research for Evolutional Science and Technology (CREST), Japan Science and Technology Agency (JST), Saitama, Japan*

Key Words: 4EBP1; *Cyanidioschyzon merolae*; rapamycin; red alga; target of rapamycin

Abbreviations: 5-FOA, 5-fluoroorotic acid; DMSO, dimethyl sulfoxide, kbp, kilobase pair; kDa, kilodalton; PEG, polyethylene glycol

The target of rapamycin (TOR) is a serine/threonine protein kinase that plays a central role in the regulation of cell growth and metabolism (Laplante and Sabatini, 2012). This protein, which is structurally and functionally conserved among eukaryotes (Virgilio and Loewith, 2006; Wullschleger et al., 2006), is found in two functionally distinct multi-protein complexes: TOR complex 1 (TORC1) and TOR complex 2 (TORC2). TORC1 regulates cell growth and metabolism in response to nutrient and energy requirements (Virgilio and Loewith, 2006; Wullschleger et al., 2006) and its functions are specifically inhibited by rapamycin (Heitman et al., 1991). TORC2, involved in the regulation of the cytoskeleton structure and spatial features of cell growth, is not inhibited by rapamycin (Virgilio and Loewith, 2006; Wullschleger et al., 2006).

Although rapamycin is a powerful tool to reveal the functions of TOR in cell growth and metabolism in eukaryotes, most land plants and algae do not show clear phenotypes against the rapamycin treatment (Crespo et al., 2005; Imamura et al., 2013; Sormani et al., 2007; Xiong and Sheen, 2012; Xiong et al., 2016) which obscures the functions of TOR in these plant lineages. To overcome this problem, we previously constructed a rapamycin-susceptible *Cyanidioschyzon merolae* F12 strain by expressing the *Saccharomyces cerevisiae* FKBP12 protein in cells of this alga (Imamura et al., 2013). To obtain the F12 strain, a plasmid harboring the *S. cerevisiae* FKBP12 gene for constitutive expression in *C. merolae* was transformed into strain M4, a uracil-auxotrophic mutant (Minoda et al., 2004). Transformants were then selected using the UMP synthase gene as a marker for uracil prototrophy (Imamura et al., 2013). Using the *C. merolae* F12 strain, we recently revealed that TOR plays a central role in triacylglycerol accumulation in microalgae (Imamura et al., 2015).

Because of its simple cell architecture and genome, low gene redundancy, and capacity for gene-knockout by homologous recombination, *C. merolae* is considered to be a good model photosynthesizing eukaryote for understanding various fundamental molecular mechanisms (Imamura et al., 2009; Kuroiwa, 1998; Matsuzaki et al., 2004). Although these features also make *C. merolae* suitable for the analysis of TOR functions using the F12 strain, no selection marker is available in F12 enabling its use as a host. Consequently, the establishment of a novel *C. merolae* strain having both rapamycin-sensitive and uracil-auxotrophic phenotypes is required to further investigate TOR functions using a molecular genetic approach.

In a recent study, we demonstrated that the T1 strain, in which the *URA5.3* gene is completely deleted, is a 5-fluoroorotic acid (5-FOA)-resistant, backgroundless host for transformation experiments (Taki et al., 2015). In the study reported here, we constructed a plasmid pKTL1, serving as a genomic knock-in cassette for insertion into the *URA5.3* gene (Fig. 1a), and obtained a novel rapamycin-susceptible *C. merolae* strain in which the *URA5.3* gene is replaced by a DNA fragment for constitutive expression of *S. cerevisiae* FKBP12 (hereafter referred to as the ScFKBP fragment) (Imamura et al., 2013). We then successfully used the isolated strain as a host strain

*Corresponding authors: Sousuke Imamura and Kan Tanaka, Laboratory for Chemistry and Life Science, Institute of Innovative Research, Tokyo Institute of Technology, Yokohama, Japan; Core Research for Evolutaional Science and Technology (CREST), Japan Science and Technology Agency (JST), Saitama, Japan.
E-mail: simamura@res.titech.ac.jp kntanaka@res.titech.ac.jp

None of the authors of this manuscript has any financial or personal relationship with other people or organizations that could inappropriately influence their work.

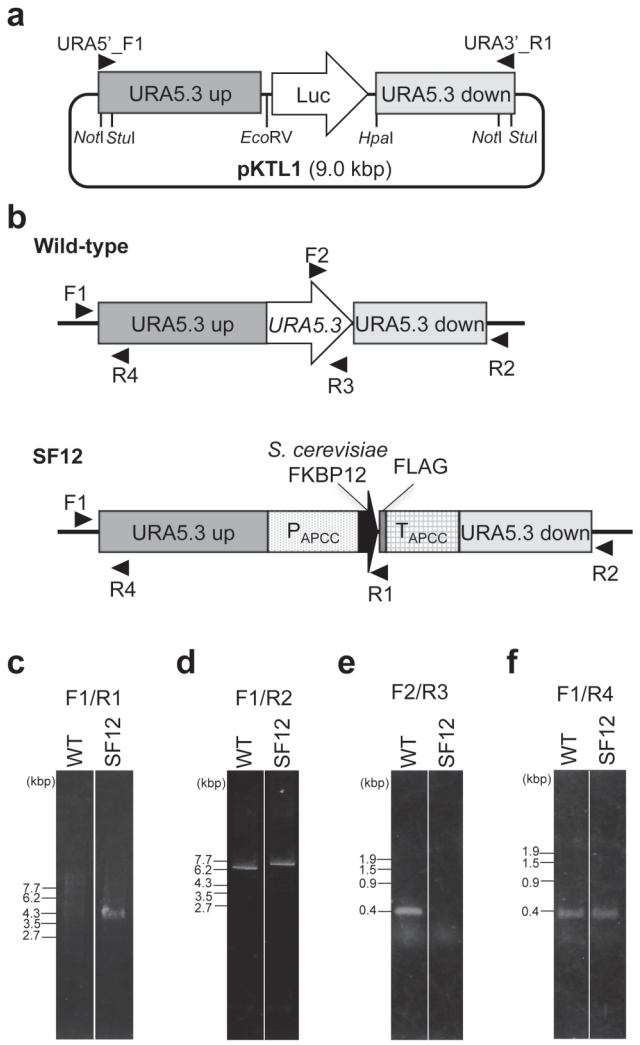

Fig. 1. Construction of the *Saccharomyces cerevisiae* FKBP12 expression strain.

(a) Schematic representation of pKTL1. "*URA5.3* up" and "*URA5.3* down" respectively denote regions upstream and downstream of *URA5.3*. Luc indicates the coding region of the luciferase gene in pGL3-Basic. The position of primers URA5′_F1 and URA3′_R1, used for PCR amplification of the DNA fragment for the transformation experiment, are indicated by arrowheads. *Eco*RV and *Hpa*I are unique restriction sites recognized by each restriction enzyme. Each two *Not*I and *Stu*I recognition sequences is located at the 5′-end of *URA5.3* up and the 3′-end of *URA5.3* down. (b) Schematics for the *URA5.3* locus in wild-type (upper) and SF12 (lower) strains. P_{APCC}, T_{APCC}, and FLAG denote the *APCC* promoter region, *APCC* terminator region, and the FLAG-tag, respectively. Arrows indicate *URA5.3* and *S. cerevisiae* FKBP12 open reading frames. The positions of primers used for the PCR analysis shown in c–f are indicated by arrowheads. F1 and R2 anneal outside of the integration region. (c–f) Confirmation of the *S. cerevisiae* FKBP12 expression strain SF12. Genomic DNAs were used as templates for PCR analyses with primer sets F1/R1 (c), F1/R2 (d), F2/R3 (e), or F1/R4 (f). The PCR products were resolved by 1.0% agarose gel electrophoresis. Positions based on a molecular size marker are indicated in kilobase pairs on the left.

to analyze TOR kinase activity *in vivo*.

The ScFKBP fragment was generated by PCR with primers pKTL1_ScFKBP_F1 (5′-AGATCTCATATGGATCTATCGGCGGTTGAAGAG-3′) and pKTL1_ScFKBP_R1 (5′-GCCCATTAGGAAGTTGCGTTCGATTGCGTCTATT-3′), with pKF-ScFKBP12 used as a DNA template (Imamura et al., 2013). All PCR amplifications in this study were carried out with KOD-Plus-Neo DNA polymerase (Toyobo). The PCR-amplified fragment was cloned into *Eco*RV/*Hpa*I-digested pKTL1 (Fig. 1a) using InFusion cloning (Clontech) to create pKTL1-ScFKBP12. pKTL1 was constructed in four steps as follows. First, to construct the plasmid pGL3_linker_plus, linker DNA was generated by annealing two synthetic oligonucleotides, Luclinker (*Kpn*)-(*Hd*) (5′-GACTAGTGGCGCGCCTCGCGAAGATCTCATATGgatatcT-3′; lowercase letters indicate *Eco*RV recognition sequences) and Luclinker(*Hd*)-(*Kpn*) (5′-AGCTAgatatcCATATGAGATCTTCGCGAGGCGCGCCACTAGTCGTAC-3′; lowercase letters indicate *Eco*RV recognition sequences); this linker DNA was inserted into the *Kpn*I and *Hin*dIII site in pGL3-Basic (Promega) to give the plasmid pGL3_linker_plus harboring an *Eco*RV site in the inserted synthetic fragment. Second, to obtain two fragments upstream (–2,761 to –586, +1 as the initiation codon) or downstream (1,393 to 3,394) of the *URA5.3* locus, PCR was carried out using *C. merolae* genomic DNA as a template and the following primers: URA_-2761F (5′-GCCCACCACGAGCGTACTG-3′) and URA_-586R (5′-TTAAATATAGTTTACCAAAAATCCATCCAG-3′) for the upstream fragment, and *Hpa*I_URA_1393F (5′-aacTTCCTAATGGGCAGAAGCAAGCG-3′; lowercase letters indicate bases added to retain the *Hpa*I site) and URA_3394R_*Stu*I (5′-CCCCGAggCCTGGGTGAGAGC-3′; lowercase letters indicate bases altered to insert the *Stu*I site) for the downstream fragment. Third, to construct the plasmid pGL3_linker_ura-up, the *URA5.3* upstream fragment was inserted into the blunted *Not*I site of the plasmid pGL3_linker_plus. Finally, to construct the plasmid pKTL1, the *URA5.3* downstream fragment was inserted into the *Hpa*I site of the plasmid pGL3_linker_ura-up. Mighty Mix (Takara) was used in the each ligation step according to the manufacturer's instructions. The ScFKBP fragment respectively harboring *URA5.3* upstream and downstream regions at 5′ and 3′ ends was amplified by PCR with primers URA5′_F1 (5′-GCCCACCACGAGCGTACTGC-3′) and URA3′_R1 (5′-CCCCGAGGCCTGGGTGAGAG-3′), with pKTL1-ScFKBP12 used as a DNA template. The resulting 7.1-kbp fragment was used in polyethylene glycol (PEG)-mediated transformation of wild-type cells. Transformants were then selected on modified Allen's 2 (MA2) plates (Imamura et al., 2010) containing 5-FOA and uracil following the same methods used for isolation of the T1 strain (Taki et al., 2015).

After an approximately 2-month incubation period for selection, isolates were screened by PCR using each genomic DNA as a template and two primers: F1 (5′-GGAGGGCACCTTACCAAAAG-3′) annealing outside of the integration region and R1 (5′-TCACTTGTCATCGTCATCCTTGTAATCGAT-3′). A 4.2-kbp DNA fragment was expected whenever the integration occurred as predicted (Fig. 1b, bottom). One positive isolate was identified (Fig. 1c). To confirm the replacement of chromosomal *URA5.3* with the ScFKBP fragment, further PCR analyses were performed using three different primer sets:

1) F1 and R2 (5′-GGAGTGGCCGGTTCTTAAA-3′) annealing outside of the integration region and expected

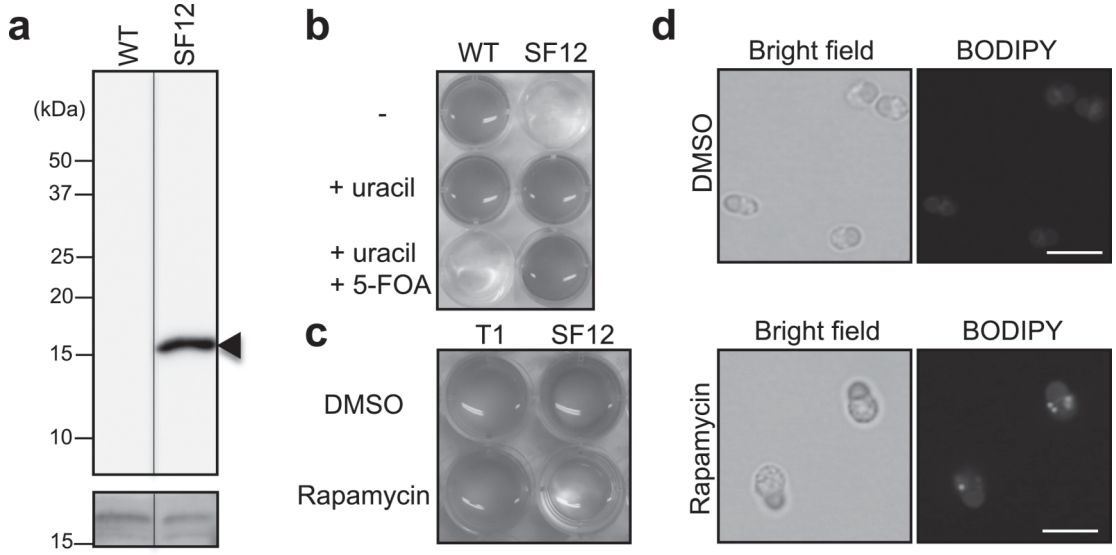

Fig. 2. Rapamycin-susceptible phenotypes of strain SF12.

(a) Results of an immunoblot analysis for *Saccharomyces cerevisiae* FKBP12 expression. Aliquots of total protein (0.9 μg each) prepared from the logarithmic growth phase of wild-type (WT) or SF12 strains were separated by 15% sodium dodecyl sulfate-polyacrylamide gel electrophoresis and analyzed by immunoblotting with a monoclonal anti-FLAG antibody. Molecular size marker positions are indicated in kDa on the left. The arrowhead indicates the expected position of the FLAG-tagged *S. cerevisiae* FKBP12 protein. After detection of a signal at approximately 18 kDa, the membrane was stained with Coomassie Brilliant Blue, which was used as a loading control (lower panel). (b) Uracil auxotrophy and 5-fluoroorotic acid (5-FOA) resistance. WT and SF12 strains were inoculated in MA2 medium or MA2 medium with uracil (0.5 mg/ml final concentration) and/or 5-FOA (0.5 mg/ml final concentration), resulting in an optical density (OD) at 750 nm (OD_{750}) of 0.1. The photograph was taken after 9 days incubation at 40°C in an Anaero Pouch with an AnaeroPack CO_2-generating agent (Mitsubishi Gas Chemical). (c) Growth inhibition caused by rapamycin treatment. T1 and SF12 strains were incubated as in (b), except that the starting OD_{750} and incubation period were 0.05 and 7 days, respectively. Rapamycin dissolved in DMSO was added to the uracil-supplemented MA2 medium to give a final concentration of 2 μM. DMSO was used as a control. (d) Lipid droplet accumulation induced by rapamycin treatment. The SF12 strain was cultured as in (c), with lipid droplet formation observed using 4,4-difluoro-1,3,5,7-tetramethyl-4-bora-3a,4a-diaza-s-indacene (BODIPY) 2 days after incubation. Bright field (left) and BODIPY staining (right) images under DMSO (upper) and rapamycin (lower) treatment conditions are shown. Bar = 5 μm.

to yield a 7.3-kbp fragment from the positive strain and a 6.3-kbp fragment from the parental wild-type strain (Fig. 1d);

2) F2 (5′-CAGTTTCATGCTTTTTGAGGATCG-3′) and R3 (5′-ACCCTTGCGCTTCAGCAGATAC-3′), with no amplification expected from the positive strain and a 0.4-kbp fragment expected from the wild-type strain (Fig. 1e); and

3) F1 and R4 (5′-GTACGGCGTTCGAAAAATAGCG-3′), with 0.4-kbp fragments expected from both positive and wild-type strains (Fig. 1f).

As shown in Figs. 1c–f, the ScFKBP fragment was integrated as expected into the *URA5.3* locus in the positive strain, the latter referred to as strain SF12.

To further confirm the replacement of *URA5.3* by the ScFKBP fragment, we examined *S. cerevisiae* FKBP12 expression, uracil auxotrophy, 5-FOA resistance, and rapamycin-susceptible phenotypes of strain SF12. Immunoblot analysis with monoclonal anti-FLAG M2 antibody (F3165; Sigma) was performed as described previously (Imamura et al., 2013), except that the lysis buffer for protein extraction contained phosphatase inhibitor cocktail (Nacalai Tesque, 100-fold dilution). This analysis confirmed the expression of the FLAG-tagged *S. cerevisiae* FKBP12 in the SF12 strain (Fig. 2a). As shown in Fig. 2b, SF12 exhibited uracil auxotrophy; in addition, it displayed 5-FOA resistance in a manner similar to the *URA5.3* deletion mutant T1 (Taki et al., 2015). In agreement with our previous observation of strain F12 (Imamura et al., 2013, 2015), SF12 strain also exhibited rapamycin-susceptible phenotypes, such as growth inhibition (Fig. 2c) and lipid droplet accumulation (Fig. 2d) in the presence of rapamycin. Lipid droplets were detected with BODIPY 505/515 (4,4-difluoro-1,3,5,7-tetramethyl-4-bora-3a,4a-diaza-s-indacene) as described previously (Imamura et al., 2015). Rapamycin-induced lipid droplet accumulation was not observed in strain T1 (data not shown). These results further support the conclusion that the *URA5.3* gene was correctly replaced by the ScFKBP fragment.

Next, to evaluate whether the SF12 strain can be used as a host strain for transformation, we cloned human eukaryotic translation initiation factor 4E-binding protein 1 (4EBP1) into pSUGA (Fujii et al., 2013) to create pSUGA-4EBP1, which was then introduced into SF12 cells to generate a 4EBP1-expressing strain. We constructed this strain because our previous *in vitro* experiment demonstrated that *C. merolae* TOR can phosphorylate human 4EBP1 (Imamura et al., 2013). It should be noted that no 4EBP1 homolog is present in *C. merolae* based on the whole genome sequence information (Matsuzaki et al., 2004; http://merolae.biol.s.u-

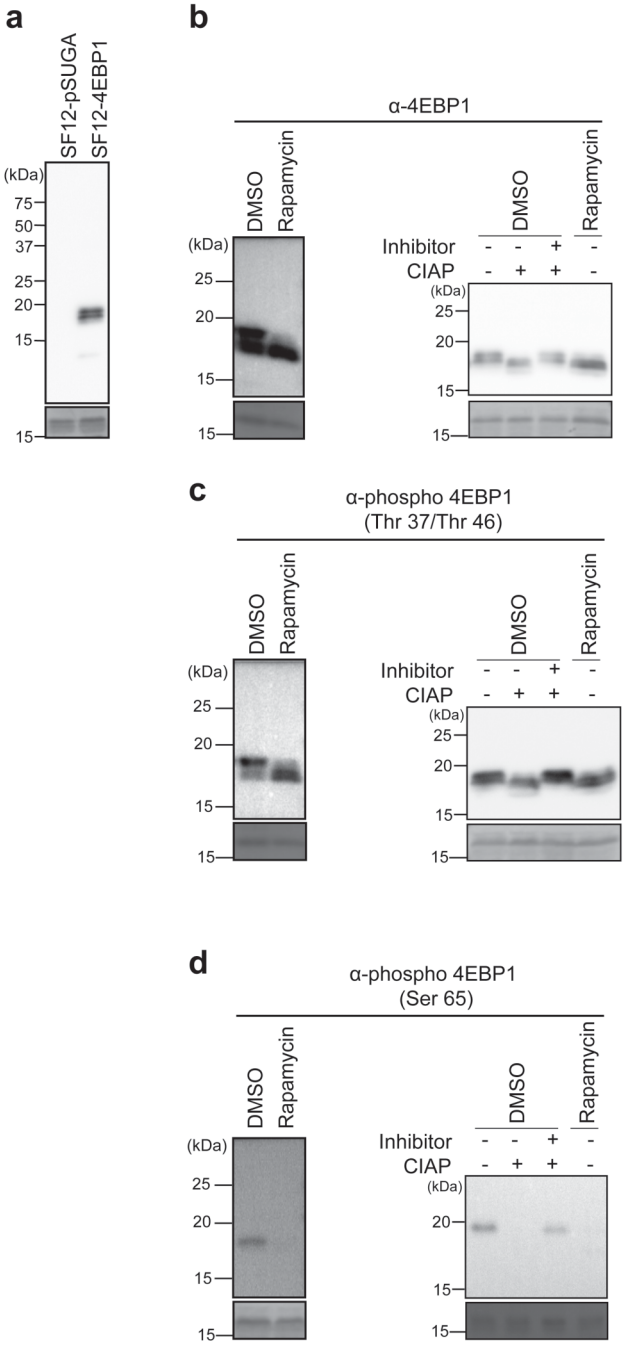

Fig. 3. Construction of a 4EBP1-expressing strain using SF12 as a host strain.

(a) Confirmation of 4EBP1 expression. Immunoblot analysis was performed with aliquots of total protein prepared from SF12-4EBP1 or SF12-pSUGA and anti-4EBP1 antibody. All other details are the same as in Fig. 2a. (b–d) Phosphorylation status of 4EBP1 under conditions of rapamycin treatment. After treating SF12-4EBP1 strains at the logarithmic growth phase (OD_{750} = 0.2–0.4) with rapamycin or DMSO for 6 h, total protein was isolated from the cells. For the phosphatase treatment experiments, the total protein (5 μg) was treated with (+) or without (–) calf intestinal alkaline phosphatase (CIAP) (TaKaRa, 10U) and/or phosphatase inhibitor cocktail (denoted as Inhibitor) (Nacalai Tesque, 25-fold dilution). The immunoblot analysis was performed with anti-4EBP1 (b), anti-phospho Thr 37/Thr 47 (c), and anti-phospho Ser 65 (d). All other details are the same as in (a).

tokyo.ac.jp). The human 4EBP1 gene was amplified with primers 4EBP1_pSUGA_F1 (5′-CGTTCGTTG-ACCCCCATGTCCGGGGGCAGCAGC-3′) and 4EBP1_pSUGA_R1 (5′-GTCGACTCTAGACCCTTA-AATGTCCATCTCAAACTG-3′), with human 4EBP1 cDNA (HG10022-M; Sino Biological) used as a template. The amplified gene was then cloned into *Sma*I-digested pSUGA using InFusion cloning. Transformants were selected by uracil autotrophy because pSUGA harbored the UMP synthase gene (Fujii et al., 2013) as a selection marker. As a control experiment, pSUGA was also introduced into SF12 cells.

Transformation with pSUGA-4EBP1 resulted in the growth of numerous colonies. Colony PCR analysis using 4EBP1_pSUGA_F1 and R1 confirmed the presence of the 4EBP1 gene in 12 independent strains (data not shown). We chose one of these strains, SF12-4EBP1, as a representative for further examination. We also isolated transformants using pSUGA and the selected one, SF12-pSUGA, for use as a control strain. To check for 4EBP1 expression in the transformant, we conducted an immunoblot analysis using anti-4EBP1 antibody (#9452; Cell Signaling Technology). As shown in Fig. 3a, two major bands of the predicted molecular size (about 18 kDa) were detected in the SF12-4EBP1 strain but not in SF12-pSUGA.

It has recently been indicated that several kinases phosphorylate 4EBP1 dependent on or independent of mammalian TOR (mTOR) (Qin et al., 2016). The phosphorylation of 4EBP1 by mTOR are well understood, and has been reported to occur in HEK 293 cells in the following order: phosphorylation of Thr 37/Thr 46 (numbered according to human 4E-BP1), followed by Thr 70 and finally Ser 65, with these phosphorylations dependent on mTOR activity (Gingras et al., 2001). This finding raises the possibility that the TOR-dependent phosphorylation status of 4EBP1 was responsible for the different band migration patterns observed above. Thus, we next subjected SF12-4EBP1 strain to 6 h of rapamycin or DMSO treatment followed by detection with anti-4EBP1 antibody and antibodies that specifically recognize the following phosphorylated amino acids of 4EBP1: phospho Thr 37 and/or Thr 46 (Thr 37/Thr 46) (#9459; Cell Signaling Technology) or phospho Ser 65 (#9451; Cell Signaling Technology). As shown in Fig. 3b, the upper band disappeared under TOR-inactivation or calf intestinal alkaline phosphatase (CIAP) treatment condition when anti-4EBP1 antibody was used. Furthermore, the effect of CIAP treatment was inhibited by the addition of phosphatase inhibitor cocktail into the reaction mixture. These results indicate that the migration of 4EBP1 is dependent on its phosphorylation status and, thus, the TOR activity. Upper and lower bands were generally visible in the presence of antibody against phospho Thr 37/Thr 46 after DMSO and rapamycin treatments, respectively (Fig. 3c). However, the detected bands with anti-phospho Thr 37/Thr 46 antibody did not disappear when the total protein was treated with CIAP (Fig. 3c), and the band patterns were similar when anti-4EBP1 antibody was used (Fig. 3b). These results indicated that anti-phospho Thr 37/Thr 46 antibody recognizes 4EBP1 protein, but did not specifically recognize

phospho Thr 37 and/or Thr 46 in *C. merolae* cells. In contrast, only the upper band was detected when anti-phospho Ser 65 antibody was used, and this band disappeared when cells were treated with rapamycin (Fig. 3d). The detected band with anti-phospho Ser 65 antibody was not visible in the total protein treated with CIAP, but the effect was blocked by the addition of phosphatase inhibitor cocktail. These results indicate that TOR activity can be monitored in *C. merolae* SF12-4EBP1 cells by observing the band migration pattern or Ser 65 phosphorylation status.

In conclusion, we have successfully constructed the rapamycin-susceptible *C. merolae* strain SF12, in which the ScFKBP fragment has been replaced by the *URA5.3* gene. Furthermore, we have demonstrated that SF12 can be used as a host strain for transformation experiments applicable to various research topics, such as the analysis of TOR-signaling regulators. As an example, SF12 was successfully applied for the construction of human 4EBP1-expressing strain SF12-4EBP1, in which TOR kinase activity can be monitored *in vivo*. Changes in TOR activity under various environmental and physiological conditions using SF12-4EBP1 would be an interesting future study focus, with the resulting data providing valuable insights into TOR functions in microalgae. Finally, the method used in this study—integration of a target gene into the *URA5.3* locus—represents a novel strategy for the molecular genetic analysis of *C. merolae*, as functional relationships between two different genes can be analyzed *in vivo*.

Acknowledgments

We thank Ms. Akiko Komatsu for her technical assistance. This work was supported by JSPS KAKENHI Grant Numbers 25440129 (to S.I.) and 15K14539 (to K.T.), MEXT KAKENHI Grant Numbers 24117521 and 26117711 (to S.I.), and the Cooperative Research Program of the Network Joint Research Center for Materials and Devices.

References

Crespo, J. L., Díaz-Troya, S., and Florencio, F. J. (2005) Inhibition of target of rapamycin signaling by rapamycin in the unicellular green alga *Chlamydomonas reinhardtii*. *Plant Physiol*., **139**, 1736–1749.

Fujii, G., Imamura, S., Hanaoka, M., and Tanaka, K. (2013) Nuclear-encoded chloroplast RNA polymerase sigma factor SIG2 activates chloroplast-encoded phycobilisome genes in a red alga, *Cyanidioschyzon merolae*. *FEBS Lett*., **587**, 3354–3359.

Gingras, A. C., Raught, B., Gygi, S. P., Niedzwiecka, A., Miron, M. et al. (2001) Hierarchical phosphorylation of the translation inhibitor 4E-BP1. *Genes Dev*., **15**, 2852–2864.

Heitman, J., Movva, N. R., and Hall, M. N. (1991) Targets for cell cycle arrest by the immunosuppressant rapamycin in yeast. *Science*, **253**, 905–909.

Imamura, S., Kanesaki, Y., Ohnuma, M., Inouye, T., Sekine, Y. et al. (2009) R2R3-type MYB transcription factor, CmMYB1, is a central nitrogen assimilation regulator in *Cyanidioschyzon merolae*. *Proc. Natl. Acad. Sci. USA*, **106**, 12548–12553.

Imamura, S., Terashita, M., Ohnuma, M., Maruyama, S., Minoda, A. et al. (2010) Nitrate assimilatory genes and their transcriptional regulation in a unicellular red alga *Cyanidioschyzon merolae*: genetic evidence for nitrite reduction by a sulfite reductase-like enzyme. *Plant Cell Physiol*., **51**, 707–717.

Imamura, S., Ishiwata, A., Watanabe, S., Yoshikawa, H., and Tanaka, K. (2013) Expression of budding yeast FKBP12 confers rapamycin susceptibility to the unicellular red alga *Cyanidioschyzon merolae*. *Biochem. Biophys. Res. Commun*., **439**, 264–269.

Imamura, S., Kawase, Y., Kobayashi, I., Sone, T., Era, A. et al. (2015) Target of rapamycin (TOR) plays a critical role in triacylglycerol accumulation in microalgae. *Plant Mol. Biol*., **89**, 309–318.

Kuroiwa, T. (1998) The primitive red algae *Cyanidium caldarium* and *Cyanidioschyzon merolae* as model system for investigating the dividing apparatus of mitochondria and plastids. *Bioessays*, **20**, 344–354.

Laplante, M. and Sabatini, D. M. (2012) mTOR signaling in growth control and disease. *Cell*, **149**, 274–293.

Matsuzaki, M., Misumi, O., Shin-I, T., Maruyama, S., Takahara, M. et al. (2004) Genome sequence of the ultra-small unicellular red alga *Cyanidioschyzon merolae*. *Nature*, **428**, 653–657.

Minoda, A., Sakagami, R., Yagisawa, F., Kuroiwa, T., and Tanaka, K. (2004) Improvement of culture conditions and evidence for nuclear transformation by homologous recombination in a red alga, *Cyanidioschyzon merolae* 10D. *Plant Cell Physiol*., **45**, 667–671.

Qin, X., Jiang, B., and Zhang, Y. (2016) 4E-BP1, a multifactor regulated multifunctional protein. *Cell Cycle*, **15**, 781–786.

Sormani, R., Yao, L., Menand, B., Ennar, N., Lecampion, C. et al. (2007) *Saccharomyces cerevisiae* FKBP12 binds *Arabidopsis thaliana* TOR and its expression in plants leads to rapamycin susceptibility. *BMC Plant Biol*., **7**, 26.

Taki, K., Sone, T., Kobayashi, Y., Watanabe, S., Imamura, S. et al. (2015) Construction of a *URA5.3* deletion strain of the unicellular red alga *Cyanidioschyzon merolae*: A backgroundless host strain for transformation experiments. *J. Gen. Appl. Microbiol*., **61**, 211–214.

Virgilio, C. D. and Loewith, R. (2006) The TOR signalling network from yeast to man. *Int. J. Biochem. Cell Biol*., **38**, 1476–1481.

Wullschleger, S., Loewith, R., and Hall, M. N. (2006) TOR signaling in growth and metabolism. *Cell*, **124**, 471–484.

Xiong, F., Dong, P., Liu, M., Xie, G., Wang, K. et al. (2016) Tomato FK506 binding protein 12KD (FKBP12) mediates the interaction between Rapamycin and target of Rapamycin (TOR). *Front. Plant Sci*., **7**, 1746.

Xiong, Y. and Sheen, J. (2012) Rapamycin and glucose-target of rapamycin (TOR) protein signaling in plants. *J. Biol. Chem*., **287**, 2836–2842.